The role of the annealing temperature on the optical and structural properties of Eu doped GaN/AlN QD

M. Peres [a], S. Magalhães [a,b], J. Rodrigues [a], M.J. Soares [a], V. Fellmann [d], A.J. Neves [a], E. Alves [b,c], B. Daudin [d], K. Lorenz [b,c], T. Monteiro [a,*]

[a] Departamento de Física and i3N, Universidade de Aveiro, Aveiro 3810-193, Portugal
[b] Instituto Tecnológico Nuclear, Sacavém 2686-953, Portugal
[c] CFNUL, Av. Prof. Gama Pinto, 1649-003 Lisboa, Portugal
[d] CEA-CNRS, Institut Nanosciences et Cryogénie, 17 rue des Martyrs, Grenoble 38054, France

ARTICLE INFO

ABSTRACT

Self assembled molecular beam epitaxy grown GaN quantum dots stacked with AlN spacers were implanted with Eu ions. The as-implanted samples were further submitted to thermal annealing treatments in nitrogen, between 1000 °C and 1200 °C. Eu^{3+} luminescence was observed in all samples with the most intense emission assigned to the $^5D_0 \rightarrow {}^7F_2$ transition in the red spectral region. The preferential excitation paths of Eu^{3+} luminescence is explored using photoluminescence excitation measurements which allow us to identify the feeding mechanisms for the Eu^{3+} ions inside the GaN quantum dots and AlN host. Optically active Eu centres in both GaN QD and AlN layers could be identified. For low implantation fluence the Eu centres inside GaN QD are dominant while for high fluences the emission arises from Eu in the AlN layers. The annealing temperature, on the other hand, does not cause any change in the local environment of the Eu-ions.

© 2010 Elsevier B.V. All rights reserved.

1. Introduction

Self assembled GaN quantum dots (QD) embedded in AlN spacer layers constitutes one of the multilayer systems particularly attractive for optoelectronic device applications [1–5]. The GaN QD photoluminescence (PL) energy is known to be dependent on the balance between the carrier's quantum confinement, strain state and giant piezoelectric effects which are responsible for the observation of GaN QD excitonic recombination above and below the bandgap of bulk GaN [6–11].

Rare earth elements have been widely used by the scientific community to optically activate nitride based materials [12–17]. Among them, Eu^{3+} luminescence due to transitions between the ^5D and ^7F multiplets have been reported in the binary and ternary $Al_xGa_{1-x}N$ ($0 \leqslant x \leqslant 1$) hosts as well as in GaN QD/AlN superlattices when doped either by ion implantation or by *in situ* growth [18–23]. Typically, the most intense intraionic luminescence in the wurtzite nitride structures is due to the $^5D_0 \rightarrow {}^7F_2$ transition which occurs in the red spectral region. In the $Al_{1-x}Ga_xN$ system it shifts from ca. 622 to 624 nm when changing the composition from GaN to AlN. With their wide bandgap the nitride hosts are very suitable

to produce highly efficient Eu^{3+} related electroluminescent devices as recently reported for MOVPE grown GaN:Eu [24]. In Eu-doped GaN and AlN layers the nonradiative carrier recombination channels severely limit the intra-$4f^6$ luminescence efficiency, which is expected to be surpassed with the incorporation of Eu^{3+} in GaN QD due to the strong confinement of the carriers in the dots and the expected decrease of the nonradiative decay paths [25]. In GaN epilayers implanted with Eu the luminescence intensity was found to increase strongly with annealing temperature [26].

The purpose of the present article is to analyse the effects of the increasing post-implant annealing temperature on the optical and structural properties of Eu-doped GaN QD/AlN SL. Photoluminescence (PL) and PL excitation (PLE) of the SL annealed at temperatures above 1000 °C is carried out to evaluate the role of the annealing temperature on excitation mechanisms of the Eu^{3+} emission in the SL structures implanted with different fluences (1×10^{13} and 1×10^{15} ions cm^{-2}).

2. Experimental

Two sets of GaN QD/AlN SL samples (#987 and #989) were grown by molecular beam epitaxy (MBE) as described elsewhere [4].

The 20 periods SL structures were implanted at room temperature (RT) with 300 keV Eu ions with fluences of 1×10^{13} and

* Corresponding author. Tel.: +351 234 370 824; fax: +351 234 378 197.
E-mail address: tita@ua.pt (T. Monteiro).

Table 1
Samples characteristics.

Sample no.	Implanted fluence (Eu ions cm^{-2})	Post-implant annealing temperature (°C)
#987	1×10^{15}	As-implanted
#987 (a)	1×10^{15}	1000
#987 (b)	1×10^{15}	1100
#987 (c)	1×10^{15}	1200
#989	1×10^{13}	As-implanted
#989 (a)	1×10^{13}	1000
#989 (a$_2$)	1×10^{13}	1000 + 1200

1×10^{15} ions cm^{-2}. Post-implant annealing was performed between 1000 °C and 1200 °C in flowing N$_2$ at 1 bar pressure and placing a piece of AlN/sapphire face to face with the samples as a proximity cap. While sample 987 (high fluence) was cut into several pieces and annealed at different temperatures an isochronous annealing was performed for sample 989 (low fluence). The samples characteristics are described in Table 1. Besides the SL structures an additional ~500 nm thick AlN layer implanted with 1×10^{15} ions cm^{-2} and annealed at 1000 °C under the same conditions was used for comparison.

High resolution X-ray diffraction (HR-XRD) was performed using CuK$_{\alpha 1}$ radiation on a D8Discover system from Bruker-AXS using a Göbel mirror, an asymmetric 2-bounce Ge(220) monochromator, and a 0.1 mm width slit placed in front of a scintillation detector.

Steady state PL measurements were carried out between 14 K and RT using the 325 nm line of a cw He–Cd laser or a 1000 W Xe lamp coupled to a monochromator as excitation sources. The used excitation energies are below the AlN bandgap. For the PLE measurements the emission monochromator was set in the Eu^{3+} emission lines and in the GaN QD excitonic recombination and the excitation wavelength was scanned up to 240 nm. The spectra were corrected to the lamp and optics.

3. Results and discussion

3.1. Low temperature PL

Fig. 1 shows the 14 K PL spectra of the red Eu^{3+} emission for the GaN QD SL samples implanted with higher and lower fluences submitted to post-implant thermal annealing treatments at different temperatures. For the #987 SL annealed at 1000 °C the $^5D_0 \rightarrow {}^7F_2$ transition is peaked nearby 624 nm and exhibits three nearly resolved lines due to the splitting of the $^7F_2$ energy level by the electric field produced through the crystalline environment. A similar splitting of the Eu^{3+} emission is found for the ions inside the AlN layer [18], being the luminescence peaked in the same spectral region. The fact that the $^5D_0 \rightarrow {}^7F_2$ transition occurs at similar wavelength in AlN and SL samples suggests that the Eu^{3+} emission for the #987 SL could take place from the AlN host (spacer, buffer or capping layer). However, it is worth mentioning that the intensity ratio of the components differs from the ones detected for the AlN:Eu layer. Differences in the fine structure intensity ratios were previously reported for GaN:Eu layers where different Eu-related centres were identified [23]. Following the same arguments the variability of the intensity ratios in our SL samples may be explained by assuming that different site symmetries and/or environment of the Eu^{3+} ions in the GaN QD/AlN structures occur when compared with AlN layers. However, as for the AlN layers only one optical active centre was found so far and wavelength selective measurements of the SL samples (see below) do not show evidence of multiple sites, the most likely explanation for this difference should be related with the different strain states for the AlN host in the SL samples. Further increase in the annealing temperature between 1000 °C and 1200 °C (Fig. 1 (a)) neither changes the peak position nor alters significantly the intraionic spectral shape suggesting that higher annealing temperatures do not lead to modifications in the lanthanide ion environment. Slight changes in the relative intensities of the three main lines for different annealing temperatures are attributed to lateral inhomogeneities of the SL samples.
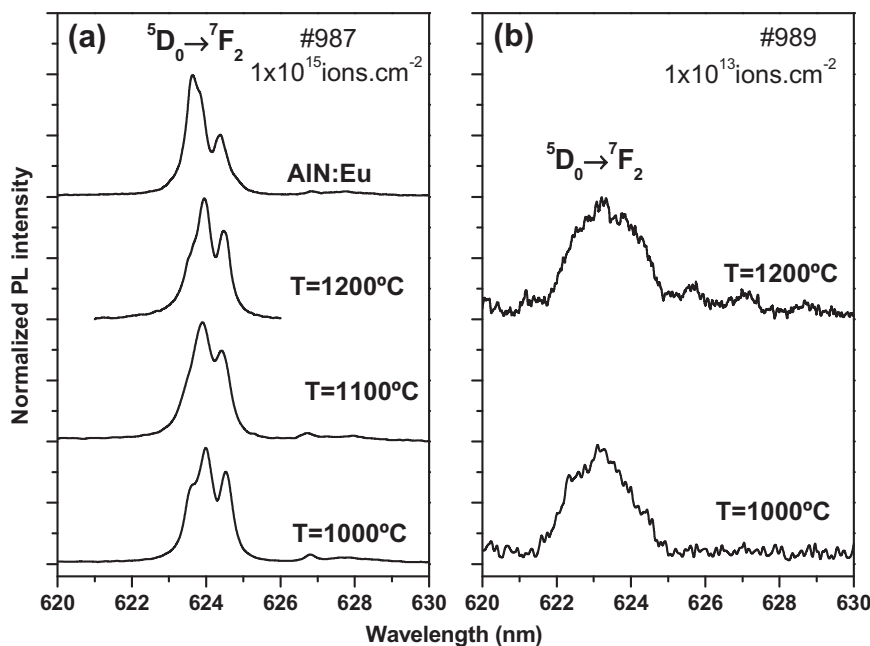

Fig. 1. $^5D_0 \rightarrow {}^7F_2$ transition of Eu^{3+} in implanted and thermally annealed GaN QD/AlN SL samples obtained at 14 K with 325 nm excitation. The spectrum of the Eu implanted thick AlN layer is shown for comparison.
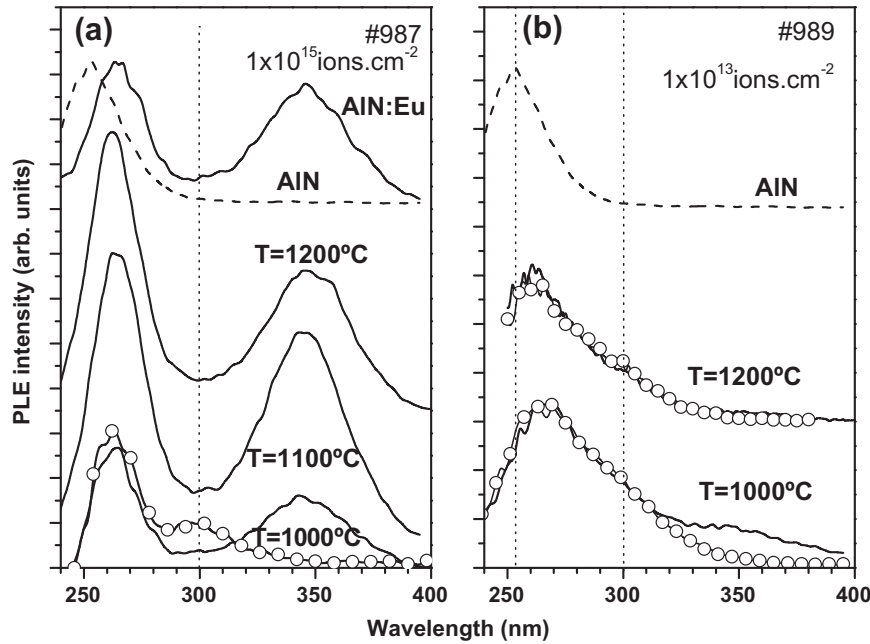
Fig. 2. Full lines: 14 K PLE spectra monitored at the $^5D_0 \rightarrow {}^7F_2$ transition of Eu^{3+} ions for the thermally annealed GaN QD/AlN SL structures and Eu doped AlN layer. Lines + symbols: 14 K PLE spectra monitored at the band maximum of GaN QD excitonic recombination. Dashed lines: PLE spectra monitored at 400 nm defect-related band in an as-grown AlN layer.

A totally distinct $^5D_0 \rightarrow {}^7F_2$ emission is measured for sample #989. Though with low intensity the Eu^{3+} luminescence is now slightly shifted to shorter wavelengths as expected for the observation of the transition in the GaN host. The transition is peaked at 623.2 nm close to the wavelength value found for the Eu^{3+} emission in *in situ* doped GaN QD [19]. The small discrepancy could be due to different distribution of strain in the SL. The measured PL suggests that for the low fluence implanted samples the Eu^{3+} emission arose mainly from the ions inside the GaN QD. Also, the thermal stability of the intraionic emission against the annealing temperature is seen to be constant. As for the high fluence samples no changes in the spectral shape are found for different annealing temperatures.

3.2. Low temperature PLE

Fig. 2 shows the low temperature PLE spectra monitored at the Eu^{3+} $^5D_0 \rightarrow {}^7F_2$ transition for the studied samples. Independently of the annealing temperature, for the SL implanted with higher fluence (Fig. 2(a)) two excitation bands with maxima at $\sim$265 nm and $\sim$345 nm are identified. For comparison purposes the PLE of an AlN:Eu layer is also shown. Similar excitation bands were previously reported in Eu-implanted AlN layers [20]. More recently, Wang et al. [18], assign the $\sim$265 nm and $\sim$345 nm excitation bands (labelled as X_2 and X_1 respectively) to the creation of core-excitonic complexes of Eu emitting centres. The observation of the X_2 and X_1 excitation bands for the high-fluence implanted GaN QD/AlN SL structures supports the conclusion that the Eu^{3+} luminescence arises from the AlN host. Moreover, the absence of spectral modifications means that no changes in the Eu^{3+} excitation paths are promoted with increasing annealing temperatures and strongly suggests that no changes on the ion environment in the AlN host occurs.

For the SL implanted with lower fluence (Fig. 2(b)) the main excitation of the Eu^{3+} emission occurs via an asymmetric band starting nearby 350 nm and peaked $\sim$265 nm. The band has a pronounced shoulder at $\sim$300 nm and the X_1 excitation band at

345 nm band is observed though with low intensity. The shoulder at $\sim$300 nm is completely absent in the high-fluence implanted SL when the PLE is monitored at Eu^{3+} emission.

In order to understand better the different physical mechanisms which could be involved in the excitation of the Eu^{3+} ions in both low and high-fluence implanted and annealed samples we must consider potential excitation mechanisms from the individual layers that constitute the SL. In this case a comparison with the PLE spectra of the GaN QD excitonic recombination as well as the PLE
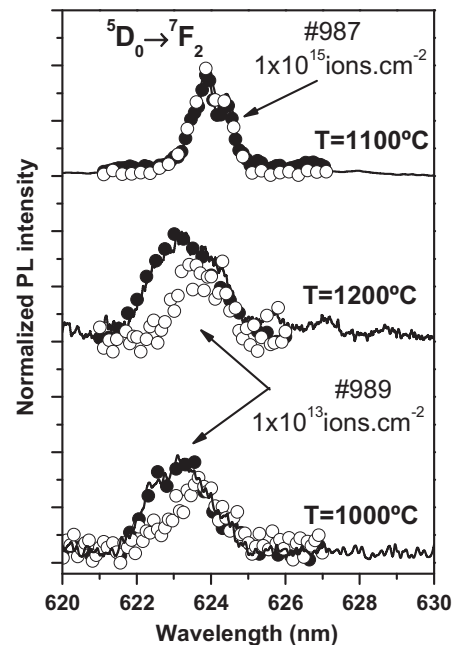

Fig. 3. Full lines: $^5D_0 \rightarrow {}^7F_2$ transition of Eu^{3+} in implanted and thermally annealed GaN QD/AlN SL samples obtained at 14 K with 325 nm excitation. Open symbols: spectra obtained with 350 nm excitation. Full symbols: spectra obtained with 265 nm excitation.
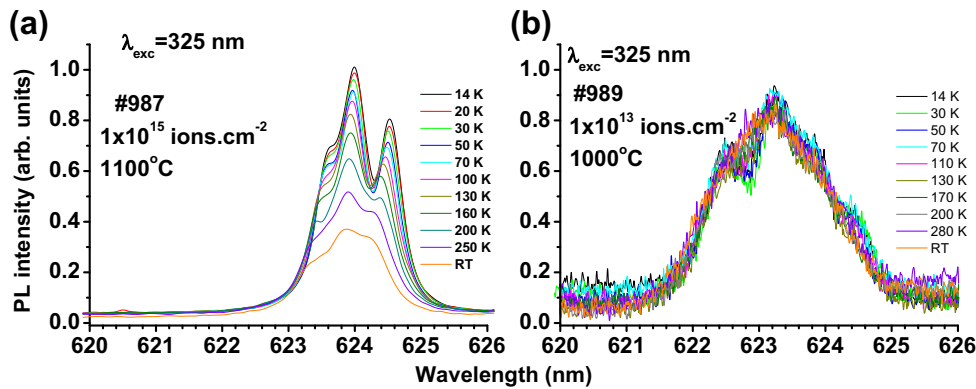
Fig. 4. Temperature dependent Eu^{3+} PL spectra obtained with 325 nm excitation for samples #987 and #989.

from optically active centres in the undoped AlN layer must be taken into account. In that sense two additional PLE spectra are shown in Fig 2(a): one monitored at the band maxima of the GaN QD excitonic recombination (at ~465 nm) in sample #987 and the other one monitored at ~400 nm in the AlN layer which corresponds to the PL maximum of a defect related emission band in the undoped AlN layer. The origin of this frequently observed defect band is of disputed origin possibly related to a donor–acceptor pair transitions involving Al vacancies [27]. As shown in Fig. 2(a) the GaN QD excitonic recombination is mainly excited via two bands at ~265 nm and ~300 nm. The low energy excitation band is likely to be due to the GaN QD excited states [28]. For the case of the high energy excitation band we must consider that the excitation of QD is achieved via the defect band seen in undoped AlN giving rise to the excitation band at ca. 250 nm when monitored at the maximum of this defect emission peak. Comparing the PLE spectra with the ones performed on the Eu^{3+} luminescence suggests that in the SL we must account for the overlapping of several excitation bands such as those related with the X_1 and X_2 bands in AlN [18,20], the defects in AlN and the excited states of the GaN QD. From the PLE data we can assume that for the SL implanted with higher fluence (#987) the Eu^{3+} emission is mainly fed by the X_1 and X_2 excitation bands although we cannot exclude that the intraionic emission could in part be excited via the ~250 nm band from the AlN-related defect levels. For the SL implanted with lower fluence (#989) and besides the X_2 excitation band and the ~250 nm band from AlN-related defect levels, the Eu^{3+} emission is excited via the absorption through the excited states of the GaN QD, the asymmetric band near 300 nm.

3.3. Selective excited PL

Further information on the Eu^{3+} ion host location in the post-implant thermally annealed GaN QD/AlN SL can be obtained from wavelength dependent PL measurements. Low temperature PL measurements were performed by exciting the two sets of SL samples at 265 nm (via X_2 and AlN-defect related excitation bands) and 350 nm (via the X_1 excitation band). The corresponding spectra are shown in Fig. 3 overlapped with the ones acquired with 325 nm excitation. For samples implanted with high fluence no spectral changes are detected on the $^5D_0 \rightarrow {}^7F_2$ transition when the Eu^{3+} emission is fed by the X_2 and X_1 excitation bands. However, for samples implanted with lower fluence a spectral shift for the $^5D_0 \rightarrow {}^7F_2$ transition is identified. With 265 nm and 325 nm excitation (matching the excited levels absorption of the GaN QD and AlN defect band) the Eu-related centre is populated in the same way as the GaN QD excitonic recombination. On the other hand, when the SL are excited at 350 nm, (the X_1 band in AlN) the $^5D_0 \rightarrow {}^7F_2$ transition is shifted to lower energies, nearby the 624 nm typical for

Eu^{3+} recombination in the AlN host. The data indicate that for the #989 SL Eu^{3+} luminescence from both hosts (GaN QD and AlN layers) can be recognized.

3.4. Temperature dependent PL

Fig. 4 shows the temperature dependent PL spectra of the implanted and annealed #987 and #989 SL structures. The spectra were obtained with 325 nm excitation which corresponds to both the X_1 and GaN QD excited states excitation bands. From the intensity variation of the $^5D_0 \rightarrow {}^7F_2$ transition, different thermal quenching processes are evidenced. For samples implanted with higher fluence an overall decrease of the luminescence intensity is seen between 14 K and RT while for samples implanted with lower fluence, preferentially excited via the same pathways as the GaN QD excitonic recombination, an almost temperature-independent Eu^{3+} luminescence is identified. This result is in agreement with the one previously reported for *in situ* doped GaN QD [19] and is an additional indication that the dominant Eu^{3+} luminescence in the low fluence samples arises from Eu centres inside GaN QD. Despite the fact that the major fraction of the Eu^{3+} are incorporated in the AlN host [22] the observation of a dominant emission from Eu ions inside the GaN QD suggests a higher excitation efficiency.

3.5. Structural analysis

The SL samples crystal quality was analysed by XRD 002 $2\theta - \omega$ scans. For 1000 °C annealing, results were reported previously for #989 samples [22]. A large number of SL peaks confirms the good crystal quality of the as-grown as well as the implanted and annealed samples. An expected c-lattice parameter expansion was found for the high-fluence implanted samples partly reversed by the annealing. On the other hand, the samples implanted with lower fluence (#989), did not reveal any lattice expansion after implantation and the XRD curves after implantation and annealing are identical to the as-grown samples indicating that the QD remain with good crystalline quality after the implantation and annealing. The retention of the good crystalline quality of the GaN QD/AlN SL structure seems to be fundamental to ensure the optical activation of the Eu^{3+} ions inside the GaN QD as we have proven by optical means. Increasing the annealing temperature up to 1200 °C did not change the measured XRD 002 $2\theta - \omega$ scans.

4. Conclusions

We have shown that in Eu-implanted GaN QD/AlN SL samples the post-growth thermal annealing between 1000 °C and 1200 °C activates the Eu^{3+} luminescence in the SL structures. For the set of samples implanted with higher fluence the intraionic emission

was seen to arise from AlN layers (buffer, spacer or capping). In this case the Eu^{3+} emission is mediated via the X_2 and X_1 excitation bands at 265 nm and 350 nm. Furthermore, temperature dependent PL studies show that the intraionic luminescence intensity drops between 14 K and RT due to competing nonradiative processes. For the high-fluence implanted samples XRD measurements show an expansion of the average SL c-lattice parameter after implantation. Thermal annealing at 1000 °C removes partially the lattice radiation damage which seems to be crucial to activate the Eu^{3+} luminescence of the Eu ions inside the SL, however, higher annealing temperatures do not lead to further structural recovery of the crystal.

In the SL samples implanted with lower fluence and submitted to post-implant thermal annealing, XRD 002 $2\theta - \omega$ curves remain unchanged by implantation and annealing suggesting that the QD remain of good quality. The emission of the Eu^{3+} ions is characterized by a broadening of the $^5D_0 \rightarrow \,^7F_2$ transition lines and the peak position is shifted to shorter wavelengths compared to the high fluence samples. In this case the excitation paths of the Eu^{3+} emission are equal to those populating the excitonic recombination of the quantum dots suggesting that the dominant optically active Eu centre is located inside the GaN QD. In addition a second Eu-related centre can be identified arising from Eu^{3+} inside the AlN host and preferentially excited at 350 nm. The Eu^{3+} emission is very weak when compared with the GaN QD excitonic recombination and practically no changes in the intraionic emission intensity was seen with increasing annealing temperature suggesting that a maximum of the Eu^{3+} ions activation was already reached for 1000 °C. In this context it is interesting to note that a rough estimate of the areal densities of QD and Eu indicates that in average the number of Eu ions incorporated inside QD is only ~0.1–0.2 ions per QD. The total number of Eu ions incorporated in AlN layers is about 10 times higher than that inside QD. A persistent Eu^{3+} luminescence was seen between 14 K and RT which is the expected behaviour for a luminescence that is fed by carriers that are strongly confined in the dots. Increasing the annealing temperature does not change the ion crystalline environments in both sets of samples.

Acknowledgements

References

[1] T. Steiner (Ed.), Semiconductor Nanostructures for Optoelectronic Applications, Artech House Inc., 2004.
[2] H. Morkoç (Ed.), Handbook of Nitride Semiconductors and Devices, Wiley-VCH, 2008.
[3] B. Daudin, F. Widmann, G. Feuillet, Y. Samson, M. Arley, J.L. Rouvière, Phys. Rev. B 56 (1997) R7069.
[4] N. Gogneau, D. Jalabert, E. Monroy, T. Shibata, M. Tanaka, B. Daudin, J. Appl. Phys. 94 (2003) 2255.
[5] J. Brault, T. Huault, F. Natali, B. Damilano, D. Lefebvre, M. Leroux, M. Korytov, J. Massies, J. Appl. Phys. 105 (2009) 033519.
[6] G. Sarusi, O. Moshe, S. Khatsevich, D.H. Rich, B. Damilano, Phys. Rev. B 75 (2007) 075306.
[7] F. Widmann, J. Simon, B. Daudin, G. Feuillet, J.L. Rouvière, N.T. Pelekanos, G. Fishman, Phys. Rev. B 58 (1998) R15989.
[8] B. Damilano, N. Grandjean, F. Semond, J. Massies, M. Leroux, Appl. Phys. Lett. 75 (1999) 962.
[9] F. Widmann, J. Simon, N.T. Pelekanos, B. Daudin, G. Feuilleta, J.L. Rouvière, G. Fishman, Microelectron. J. 30 (1999) 353.
[10] M. Peres, A.J. Neves, T. Monteiro, S. Magalhães, E. Alves, K. Lorenz, H. Okuno-Vila, V. Fellmann, C. Bougerol, B. Daudin, Phys. Stat. Sol. (B) 247 (2010) 1675.
[11] F. Guillot, E. Bellet-Amalric, E. Monroy, M. Tchernycheva, L. Nevou, L. Doyennette, F.H. Julien, Le Si Dang, T. Remmele, M. Albrecht, T. Shibata, M. Tanaka, J. Appl. Phys. 100 (2006) 044326.
[12] H.J. Lozykowski, W.M. Jadwisienczak, I. Brown, Appl. Phys. Lett. 74 (1999) 1129.
[13] A.J. Steckl, J.M. Zavada, MRS Bull. 24 (1999) 33.
[14] D.S. Lee, J. Heikenfeld, R. Birkhahn, M. Garter, B.K. Lee, A.J. Steckl, Appl. Phys. Lett. 76 (2000) 1525.
[15] T. Monteiro, C. Boemare, M.J. Soares, R.A.S. Ferreira, L.D. Carlos, K. Lorenz, R. Vianden, E. Alves, Phys. B Conden. Matter 308 (2001) 22.
[16] M. Peres, S. Magalhães, N. Franco, M.J. Soares, A.J. Neves, E. Alves, K. Lorenz, T. Monteiro, Microelectron. J. 40 (2009) 377.
[17] I.S. Roqan, K.P. O'Donnell, R.W. Martin, P.R. Edwards, S.F. Song, A. Vantomme, K. Lorenz, E. Alves, M. Boćkowski, Phys. Rev. B 81 (2010) 085209.
[18] K. Wang, K.P. O'Donnell, B. Hourahine, R.W. Martin, I.M. Watson, K. Lorenz, E. Alves, Phys. Rev. B 80 (2009) 125206.
[19] Y. Hori, X. Biquard, E. Monroy, D. Jalabert, F. Enjalbert, L.S. Dang, M. Tanaka, O. Oda, B. Daudin, Appl. Phys. Lett. 84 (2004) 206.
[20] H.J. Lozykowski, W.M. Jadwisienczak, Phys. Stat. Sol. (B) 244 (2007) 2109.
[21] M. Peres, A.J. Neves, T. Monteiro, S. Magalhães, N. Franco, K. Lorenz, E. Alves, B. Damilano, J. Massies, A. Dussaigne, N. Grandjean, J. Nanosci. Nanotechnol. 10 (2010) 2473.
[22] S. Magalhães, M. Peres, V. Fellmann, B. Daudin, A.J. Neves, E. Alves, T. Monteiro, K. Lorenz, J. Appl. Phys. 108 (2010) 84306.
[23] K. Wang, R.W. Martin, K.P. O'Donnell, V. Katchkanov, E. Nogales, K. Lorenz, E. Alves, S. Ruffenach, O. Briot, Appl. Phys. Lett. 87 (2005) 112107.
[24] A. Nishikawa, T. Kawasaki, N. Furukawa, Y. Terai, Y. Fujiwara, Appl. Phys. Exp. 2 (2009) 71004.
[25] J.M. Gérard, O. Cabrol, B. Sermage, Appl. Phys. Lett. 68 (1996) 3123.
[26] K. Lorenz, U. Wahl, E. Alves, S. Dalmasso, R.W. Martin, K.P. O'Donnell, S. Ruffenach, O. Briot, Appl. Phys. Lett. 85 (2004) 2712.
[27] T. Schulz, Ph.D. Dissertation, Tech. Univ. Berlin, (2010).
[28] B.J. Kwon, J.S. Hwang, H.S. Kwack, Y.H. Cho, N. Gogneau, B. Daudin, L.S. Dang, Phys. Stat. Sol. (C) 3 (2006) 2056.